Appl. Phys. A 66, S565–S568 (1998)

Applied Physics A
Materials
Science & Processing

Dewetting of thin collagenous precursor films

M. Mertig, U. Thiele, J. Bradt, D. Klemm, W. Pompe

Institut für Werkstoffwissenschaft, Technische Universität Dresden, D-01062 Dresden, Germany
(Fax: +49-351/463-1422, E-mail: mertig@tmfs.mpgfk.tu-dresden.de)

Received: 25 July 1997/Accepted: 1 October 1997

Abstract. We have studied structure formation of thin monomeric collagen films prepared by spin coating on hydrophobic highly oriented pyrolytic graphite substrates. The biomolecular coatings have been investigated by scanning force microscopy. Pattern formation takes place as the result of dewetting of the liquid precursor initiated by pore nucleation in the drying film. The growth of pores leads to an accumulation of collagen monomers along the perimeter of the dry patches formed. Depending on the evaporation velocity of the solvent, different well-defined film morphologies have been observed. The pore radius distribution function exhibits two well-separated peaks, indicating the occurrence of two distinct dewetting mechanisms: heterogeneous pore nucleation and spinodal dewetting. The distribution function of the pores initiated by heterogeneous nucleation is analysed in detail. A model is introduced that captures the main distribution features depending on humidity.

Investigations of the wetting properties of thin liquid films on solid substrates are of great importance for various areas of science and technology. Up to now, most of the research in this field has been concentrated on the development of methods that prevent a drying liquid film from dewetting the substrate [1]. On the other hand, by making use of dewetting processes, it should also be possible to pattern films in a controlled manner. The latter is especially interesting for the development of new biocompatible implant materials with patterned biomolecular coatings, which may induce bonding between the synthetic material and the tissue [2]. The rod-like collagen I molecule ($l = 300\,\mathrm{nm}$, $d = 1.5\,\mathrm{nm}$) provides cell adhesion sites for osteoblasts which are responsible for bone synthesis. Therefore, the study of the interaction between the mediating collagen film and implant surfaces is of great importance. Structure formation of monomeric collagen I films on substrates with different wetting properties has recently been investigated by Mertig et al. [3].

Dewetting of thin nonvolatile liquid films has been extensively investigated during the last few years [4–10]. It has been found that dewetting takes place in three successive phases: rupture of the film, growth of pores resulting in a polygonal network of liquid rims, and evolution of the rims. Two different mechanisms are taken into consideration as the cause of film rupture: (1) nucleation of holes in the thin film and subsequent growth of dry patches [5, 11] and (2) based on a hydrodynamic theory for viscous or viscoelastic thin liquid films, spontaneous growth of surface undulations under the influence of van der Waals long-range forces [12–14]. The latter theoretical models predict that spontaneous film rupture occurs with a characteristic wavelength that scales with the square of the film thickness: $\lambda \sim 1/h^2$. With these two mechanisms, the experimental observations have been discussed controversially. In investigations of dewetting of polystyrene films on silicon substrates a $1/h^4$ dependence of the pore density on the film thickness has been found, which was taken as evidence for the film surface instability [7, 8]. On the other hand, by taking into account the random spatial distribution of pores, it has been concluded that the dominant rupture process is the nucleation at defects [10]. Recently, the simultaneous occurrence of both rupture modes has been reported for the dewetting of thin liquid metal films on fused silica substrates during short-pulse laser heating [9]. Pores at two clearly separated length scales have been observed, where the smaller ones, originating from the spinodal dewetting, exhibit both a $\lambda \sim 1/h^2$ dependence and a well-developed short-range order [9, 10]. The lateral profile of the energy density of the laser pulse, used to anneal the film locally, allows different stages of both mechanisms to be observed on one and the same sample.

In this paper, we report on dewetting of an evaporating precursor film. The precursor consists of collagen monomers dissolved in acetic acid. Films with an initial thickness of about 10 μm [3] are prepared by spin-coating on a flat substrate. Evaporation of the solvent causes a decrease in the film thickness with time. During drying, the film ruptures and pores are formed. The growth of pores leads to an accumulation of collagen monomers along the perimeter of the dry patches formed . The pores are free of collagen. The development of the pore network stops when the solvent is completely evaporated. The evaporation rate of the solvent is determined by the humidity in the film preparation chamber. Thus different stages of the dewetting process can be investigated by controlling the time the film has to develop by controlling the humidity during spin-coating. Since the diameters of the pores are much smaller than those in the dewetting

experiments discussed above, the resulting film structure is imaged by scanning force microscopy (SFM).

It should be emphasised that the main advantage of the experiment described in this article lies in its intrinsic dynamic. Evaporation drives the system to smaller film thickness. Therefore, depending on the evaporation rate both, heterogeneous nucleation of pores and spinodal dewetting, which are dominant at different film thicknesses, should occur. At a low evaporation rate, heterogeneous nucleation starting at a larger film thickness should be the dominant rupture process. In this work the humidity dependence of the pores size distribution resulting from heterogeneous nucleation is analysed. Assuming randomly distributed nucleation sites with an activation rate depending on the film thickness, we introduce a simple model for the pore size distribution, which explains qualitatively the observed data.

1 Experimental

Soluble type-I collagen from calfskin (Fluka, Buchs, Switzerland) was dissolved under stirring at 4 °C for at least 2 hours at a concentration of 0.2 mg/ml in 100 mM acetic acid (pH $\approx$ 3). In some cases the collagen monomers were denatured by warming the sample to 50 °C for 30 min. The thin collagen films were prepared by spin coating at controlled humidity at room temperature. For that, a 30 µl drop of the solution was placed on the substrate. The drop was allowed to stand for 1 min on the substrate before spinning of the substrate was started at 5000 rpm. Spinning was maintained for 1 min. As the substrate we used freshly cleaved highly oriented pyrolytic graphite (HOPG). The contact angle of the precursor on HOPG was measured to be $\Theta = 75°$. The dried monomeric collagen films were examined by SFM using a NanoScope IIIa (Digital Instruments, Santa Barbara) operated in tapping mode under ambient environmental conditions. Scanning at a scan rate of 1 Hz was performed with silicon-tip cantilevers (NanoProbe^{TM}, 125 µm) at a minimum tapping force. The statistics of the network geometry of the observed structures were analysed with the image analyser QUANTIMET 570 (Leica, Bensheim) in combination with our own analysis programs [3].

2 Results and discussion

Collagen films were prepared at humidity values between 15% and 100%. Below 90% humidity, networks of pores have been observed which are homogeneous over the sample. Above 90%, hydrodynamic instabilities of the dewetting fronts come into play, resulting in patterns with side-branches or tree-like structures. Here, we concentrate on the pattern formation below 90%. Figure 1 shows an example of four different network patterns prepared at 15%, 60%, 82%, and 88% humidity. In all cases we observe formation of bare patches on the substrate. The pores are surrounded by collagen rims. The height of the rims increases with increasing humidity. The given series of images shows that the average diameter of pores also grows with increasing humidity. At 88% (Fig. 1d) the pores in the film have grown until the rims of neighbouring pores come into contact and form one common rim, leading to a polygonal network pattern. At lower humidity (Fig. 1a and b) a network of fine-structured pores develops between the larger pores. The pore radius distribution function, derived from the used image analysis program, shows two pronounced peaks at about 30 nm and at about 100 nm. The position of the first peak does not change with humidity. However, the peak height decreases with increasing humidity. The peak vanishes at about 70% humidity. The second peak shifts towards higher mean values; its width grows with increasing humidity as well (see Table 1).

The rims of the polygonal network structures, as shown in Fig. 1d, are found to be stable. We never observed their decay into rows of small drops as usually expected for liquids

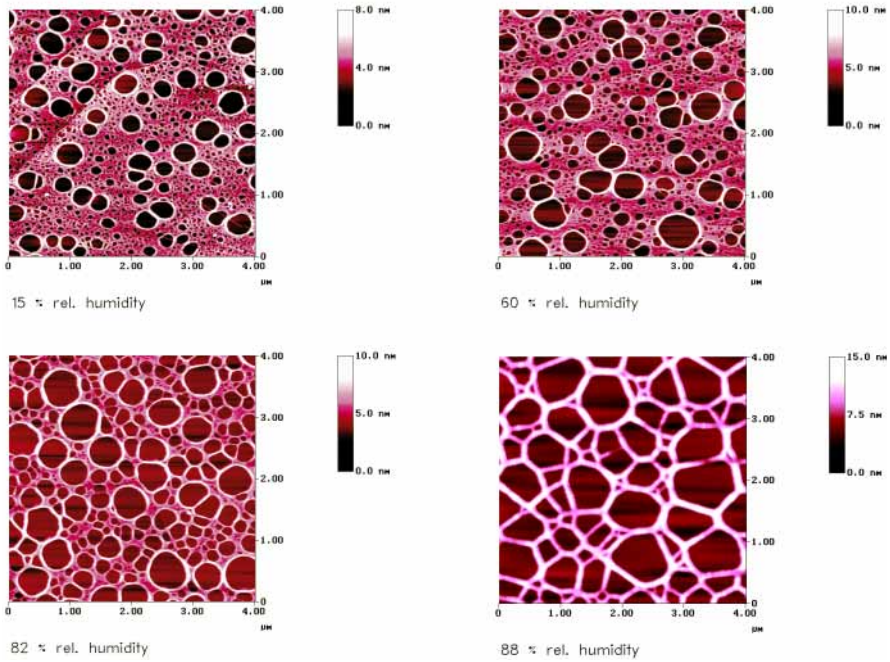

Fig. 1a–d. SFM micrographs of thin collagen films on HOPG, prepared at different humidity: **a** 15%, **b** 60%, **c** 82%, and **d** 88%. The sizes of the micrographs are 4 µm × 4 µm. The grey scales correspond to height signal ranges of 8 nm, 10 nm, 10 nm, and 15 nm, respectively. The images show cut-outs of the areas analysed for the corresponding pore size distributions

Table 1. Mean value and standard deviation of the measured pore radius distribution functions for different humidity

Humitidy/%	Mean pore radius/nm	Standard deviation/nm
15	113	30
60	117	44
82	129	53
88	214	107

owing to the Rayleigh instability [8]. The rims are stabilised by the rod-like collagen monomers, whose lengths are comparable to the characteristic diameter of the pores. That is, the mechanical strength of the molecules compensates the capillary forces that want to break up the rims. To prove this hypothesis, films have been prepared from denatured collagen solution. The length of the molecule decreases as a result of a conformational change into a random coil during denaturing at 50 °C. Figure 2 shows a film of denatured collagen prepared at 97% humidity. Here, the rims show the tendency to decay into drops. Nevertheless, the high viscosity of the precursor hinders a total rupture of the rims before the structure is completely dried up.

We suspect that the occurrence of two well-separated peaks in the pore radius distribution function indicates that two distinct mechanisms of pore formation are involved in the film structure formation. They respond differently to the change in the process parameters such as the evaporation rate of the solvent. The larger pores arise from film rupture as a result of heterogeneous nucleation. Starting with a lower probability at large film thicknesses, nucleation continues as the film is thinned by evaporation. At the same time, "earlier" nucleated pores grow. In terms of nonruptured film area, the ongoing nucleation of new pores competes with the growth of "older" pores. These two processes can be influenced by a changing humidity. At high humidity the film thickness decreases slowly; that is, pores nucleated at large film thickness grow to a large size. The nucleation rate changes only slightly, since the film thickness is altered slowly. Pore formation stops mainly because the nonruptured film area approaches zero at a finite precursor film thickness. In the case of low humidity the solvent evaporates rapidly, and nucleated pores have

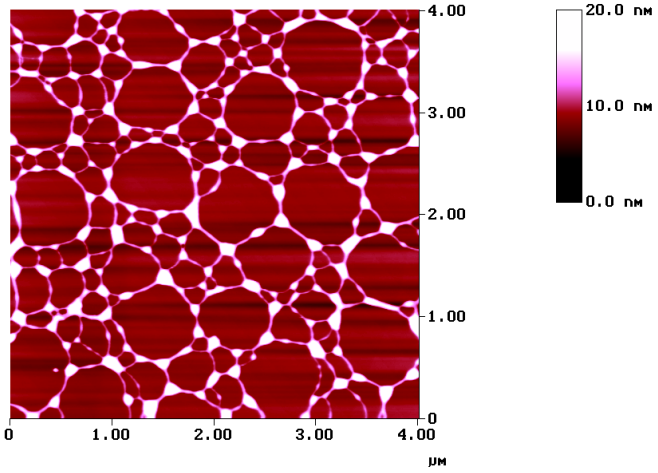

Fig. 2. Image of a thin film of denatured collagen prepared at 97% humidity. The image shows an intermediate state of the decay of the rims into droplets

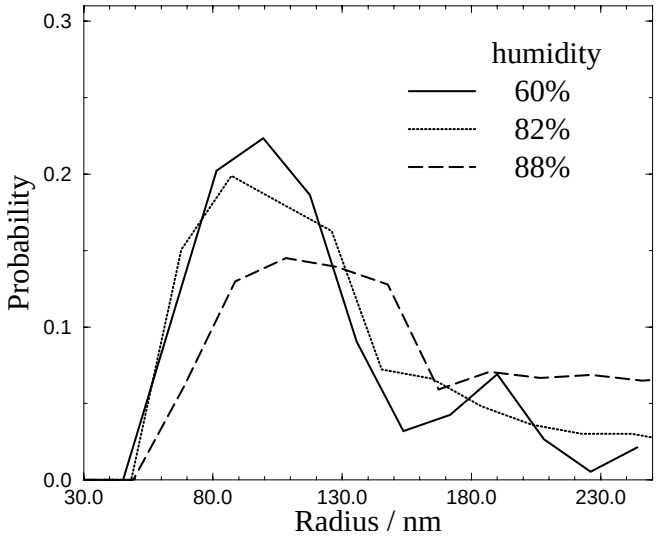

Fig. 3. Normalised distribution functions of the radii of pores initiated by heterogeneous nucleation at different humidity. All pores with $r > 50$ nm are taken into account

no time to grow to a large size. Therefore, the mean pore size is smaller at low humidity than at high humidity. Under these conditions the change in the nucleation rate is caused by both a decreasing nonruptured film area and a decreasing film thickness.

At very low humidity a large area remains nonruptured when the film thickness reaches the length scale of molecular interactions between the precursor and the substrate. For thin water films with a thickness below 100 nm, it has been observed that the apolar part of the interaction with most substrates is stabilising whereas the polar part destabilises the film [15]. The polar instability becomes important at a film thickness between 5 nm and 10 nm. The typical rupture time depends on the film thickness exponentially. When the film is driven into this thickness range the remaining precursor film ruptures practically at once with a typical wavelength of about 50 nm. This value is derived from experimental data [16, 17] by using the method developed by Sharma [15]. This gives a strong indication that the 30-nm-radius pores, correlated to the first peak in the measured radius distribution function, are caused by spinodal dewetting through polar interactions. It should be emphasised once more that the observation of spinodal dewetting in collagenous precursor films became possible only as a result of the dynamic character of the experiment.

In the following, we will concentrate on the pore radius distribution function for radii above 50 nm, as given in Fig. 3. The curves represent data for humidity values of 60%, 82%, and 88%. They are normalised with respect to the radius range shown. The images given in Fig. 1b–d are part of the analysed data. Data taken at 15% humidity are not included in Fig. 3, since the small number of large pores did not give sufficient statistics. The peak position of the distribution function shifts toward higher values with increasing humidity. Also the relative weight of the larger pore radii rises with increasing humidity. The distribution functions exhibit long tails (not shown in the figure). In Table 1 the mean radii and standard deviations of the whole distribution functions are given. Both values rise with increasing humidity.

Here we propose a simple model to describe the main features of the radius distribution function of pores generated by heterogeneous nucleation and their humidity dependency. Two processes are taken into account: nucleation and pore growth, competing with each other. To keep the model simple, interactions between the pores are neglected. Thus, circular pores are assumed to grow independently. The pore area is given by $a = \pi u^2 t^2$, where u is the velocity of the dewetting front of the pore and t is the time since the pore was nucleated. The viscosity is assumed to be constant. It has been shown that under this condition u does not depend on the film thickness [4, 6]. The nonruptured film area is $A(t) = A_0 - A_P(t)$ where A_0 is the initial film area and $A_P(t)$ is the total pore area at a time t. The pore nucleation rate per unit area is $n(t) = n_P A(t)/A_0$, where n_P is assumed to depend only on the film thickness $h(t)$. Asymptotically, n_P should fulfil the conditions: $n_P(h_0) = n_0$, where h_0 is the initial thickness at $t = 0$, and $n_P(h \to 0) = \infty$. This can be described with the time dependence of the film thickness $h(t) = h_0(1 - \nu t)$, leading to

$$n_P(t) = n_0 \, e^{\alpha \nu t/(1-\nu t)} , \qquad (1)$$

where ν is the evaporation rate and α is a fit parameter. In a linear approximation ν is proportional to $1 - H$, where H is the relative humidity. That is, ν is equal to ν_0 at zero humidity and is equal to zero at 100% humidity. H is given by $H = p_v/p_s$, where p_v is the vapour pressure and p_s is the saturation vapour pressure. Because $A_P(t)$ depends on all $n(t')$ with $t' < t$, we get the integral equation

$$n(t) = n_P\big(h(t)\big)\left(1 - \pi u^2 \int_0^t n(t')(t - t')^2 \, dt'\right) . \qquad (2)$$

The time dependence of the nucleation rate can be calculated numerically by putting (1) into (2). From here, the humidity dependence of the pore radius distribution function in the final state can be derived. Figure 4 compares the normalised distribution functions when the evaporation rate is increased relatively by a factor up to 2. The peak in the distribution function is shifted to lower radii with increasing ν, since the nucleation probability rises mainly because of film thinning. Pores nucleated at higher film thickness do not have enough time to grow to larger sizes. As a result, the peak amplitude grows and the relative number of pores with large diameters decreases. A comparison between Fig. 3 and Fig. 4 shows that the observed humidity dependencies of the mean value and the standard deviation can be qualitatively described by the model. However, it should be mentioned that the distribution function at small pore radii cannot be calculated in an adequate way with the proposed model. This is because the model neglects both the finite width of the rims around the pores and the critical radius $r_C = h/\sin\Theta$ (Θ is the contact angle) that a pore has to reach in order to grow. With these effects taken into account, the calculated distribution function should not start at zero radius but at a finite value. An improved model would also take into account interactions between pores and leads consequently to the application of the Johnson–Mehl model of stochastic geometry [18, 19]. But even within the simple model proposed in this work an important conclusion can be drawn. The qualitative correspondence between model and experimental data implies that heterogeneous nucleation takes place during all stages of film thinning. Assuming a constant nucleation rate would result within our model in a monotonously increasing pore radius distribution without any maximum. On the other hand, instantaneous nucleation at one defined thickness can also be excluded, since in this case much smaller, nearly symmetric distributions have been calculated [19].

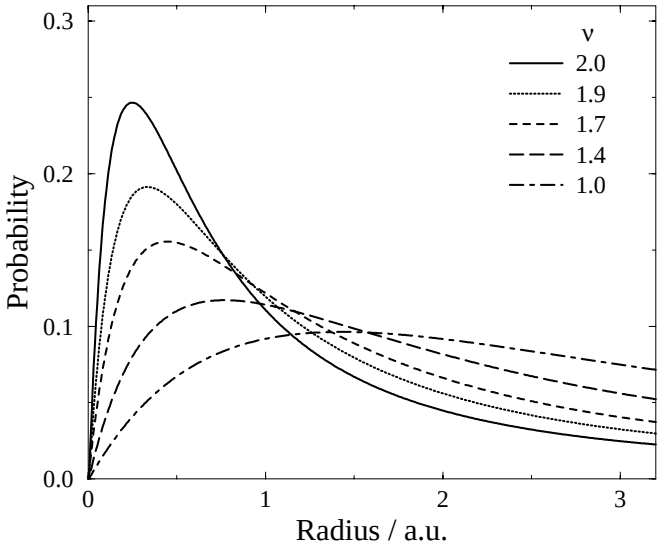

Fig. 4. Normalised pore radius distribution functions calculated for different evaporation rates by (2)

Acknowledgements. We wish to thank H. Wendrock for the assistance in the image analysis. We are grateful to P. Leiderer, M. Fischer and G. Keßler for helpful and encouraging discussions. This research was partly supported by the Bundesministerium für Bildung, Wissenschaft, Forschung und Technologie (BEO), contract No. 0310812.

References

1. R. Yerushalmi-Rozen, J. Klein, L.J. Fetters: Science **263**, 793 (1994)
2. L.L. Hench, J. Wilson: In *Advanced Series in Ceramics*, Vol. 1, ed. by M. McLare, D.E. Niesz (World Scientific, Singapore 1993) p. 1
3. M. Mertig, U. Thiele, J. Bradt, G. Leibiger, W. Pompe, H. Wendrock: Surf. Interface Anal. **25**, 514 (1997)
4. P.G. de Gennes: Rev. Mod. Phys. **57**, 827 (1985)
5. F. Brochard-Wyart, J. Daillant: Can. J. Phys. **68**, 1084 (1989)
6. C. Redon, F. Brochard-Wyart, F. Rondelez: Phys. Rev. Lett. **66**, 715 (1991)
7. G. Reiter: Phys. Rev. Lett. **68**, 75 (1992)
8. A. Sharma, G. Reiter: J. Colloid Interface Sci. **178**, 383 (1996)
9. J. Bischof, D. Scherer, S. Herminghaus, P. Leiderer: Phys. Rev. Lett. **77**, 1536 (1996)
10. K. Jacobs: PhD thesis (UFO, Allensbach 1997, ISBN 3-930803-10-0)
11. H.S. Kheshgi, L.E. Scriven: Chem. Eng. Sci. **46**, 519 (1991)
12. A. Vrij: Disc. Faraday Soc. **42**, 23 (1966)
13. E. Ruckenstein, R.K. Jain: J. Chem. Soc., Faraday Trans. 2 **70**, 132 (1974)
14. S.A. Safran, J. Klein: J. Phys. II **3**, 749 (1993)
15. A. Sharma: Langmuir **9**, 861 (1993)
16. R.J. Hunter: *Foundation of Colloid Science*, Vol. 1 (Clarendon Press, Oxford 1992)
17. J.N. Israelachvili: *Intermolecular and Surface Forces* (Academic Press, London 1992)
18. H. Hermann: *Stochastic Models of Heterogeneous Materials* (Trans Tech Publications Ltd, Zürich 1991)
19. J. Moller: Adv. Appl. Prob. **24**, 814 (1992)